

Understanding the binding of Quinoline Amines with Human Serum Albumin by Spectroscopic and Induced Fit Docking Methods

K.N. Vennila & Kuppanagounder P. Elango

To cite this article: K.N. Vennila & Kuppanagounder P. Elango (2018): Understanding the binding of Quinoline Amines with Human Serum Albumin by Spectroscopic and Induced Fit Docking Methods, Journal of Biomolecular Structure and Dynamics, DOI: [10.1080/07391102.2018.1496141](https://doi.org/10.1080/07391102.2018.1496141)

To link to this article: <https://doi.org/10.1080/07391102.2018.1496141>

 View supplementary material [↗](#)

 Accepted author version posted online: 27 Jul 2018.

 Submit your article to this journal [↗](#)

 Article views: 1

 View Crossmark data [↗](#)



Understanding the binding of Quinoline Amines with Human Serum Albumin by Spectroscopic and Induced Fit Docking Methods

K.N.Vennila and Kuppanagounder P. Elango*

*Department of Chemistry, Gandhigram Rural Institute (Deemed to be University),
Gandhigram 624 302, India*

**Corresponding author E-mail: drkpelango@rediffmail.com*

Abstract

Seven new quinoline based bioorganic compounds were prepared by solvent free synthesis and characterized using spectral techniques. The binding of these compounds with Human Serum Albumin (HSA) was investigated by multi-spectroscopic methods. The quenching of Trp fluorescence upon addition of these compounds to HSA confirmed their significant binding. The quenching analysis at three different temperatures revealed that the complex formation is static and the reaction is entropy driven, spontaneous and exothermic. Hydrogen bonds and van der Waals forces mainly contributed in the interactions as confirmed by the negative ΔH and ΔS values as well as molecular docking. The results from the CD spectroscopy indicated the minimal conformational changes of the protein upon binding with these quinoline compounds. The specific binding site and mode of interactions with HSA was also modeled using induced fit molecular docking procedure and their binding site was found to be in the interface of domains II and III, which is similar to the binding of the drug iodipamide with serum albumin.

Keywords: HSA; quinoline; fluorescence quenching; induced fit molecular docking

Introduction

Quinoline scaffold fused with various heterocycles always attract both synthetic and medicinal chemists because of its diverse chemical and pharmacological properties (Kumar et al., 2009). Compounds with this motif have been found to possess a broad range of biological activities such as anti-cancer (Afzal et al., 2015; Chan et al., 2012), anti-fungal (Musiol et al., 2006; Oliva et al., 2003), anti-malarial (Korotchenko et al., 2015) anti-tuberculosis (Adhikari et al., 2010; Lilienkamp et al., 2009; Thomas et al., 2011) anti-protozoal (Hayat et al., 2011) and anti-neoplastic (Heidary et al., 2014) inhibition of epidermal growth factor receptor (EGFR) and human epidermal growth factor receptor-2 (HER-2) kinases (Tsou et al., 2005). Few commercially available drugs containing quinoline moiety are shown in Figure 1 in which chloroquine and mefloquinone are still the most recommended for the treatment of Malaria. They are also reported to inhibit anticancer targets such as EGFR & HER2 due to its unique binding mode. Considering cell line inhibition, many quinoline derivatives are being reported as MCF-7 breast cancer cell line inhibitors with micro to nano molar IC₅₀ values (Jain et al., 2016). On the other hand, the clear understanding of interactions between quinoline derivatives and proteins would offer a basis for the future design of promising drugs (Wang et al., 2013). With this importance and as a part of our research interest, here in this article we report on the synthesis, characterization and serum binding properties of 4-aminoquinolines (**1a-g**). To exhibit all the above mentioned bioactivities *in vivo*, the ligands should be transported to the desired site, which will be done by the carriers, the serum albumin. Albumin is the main extra cellular protein and is highly concentrated and abundant in blood plasma and hence the present study.

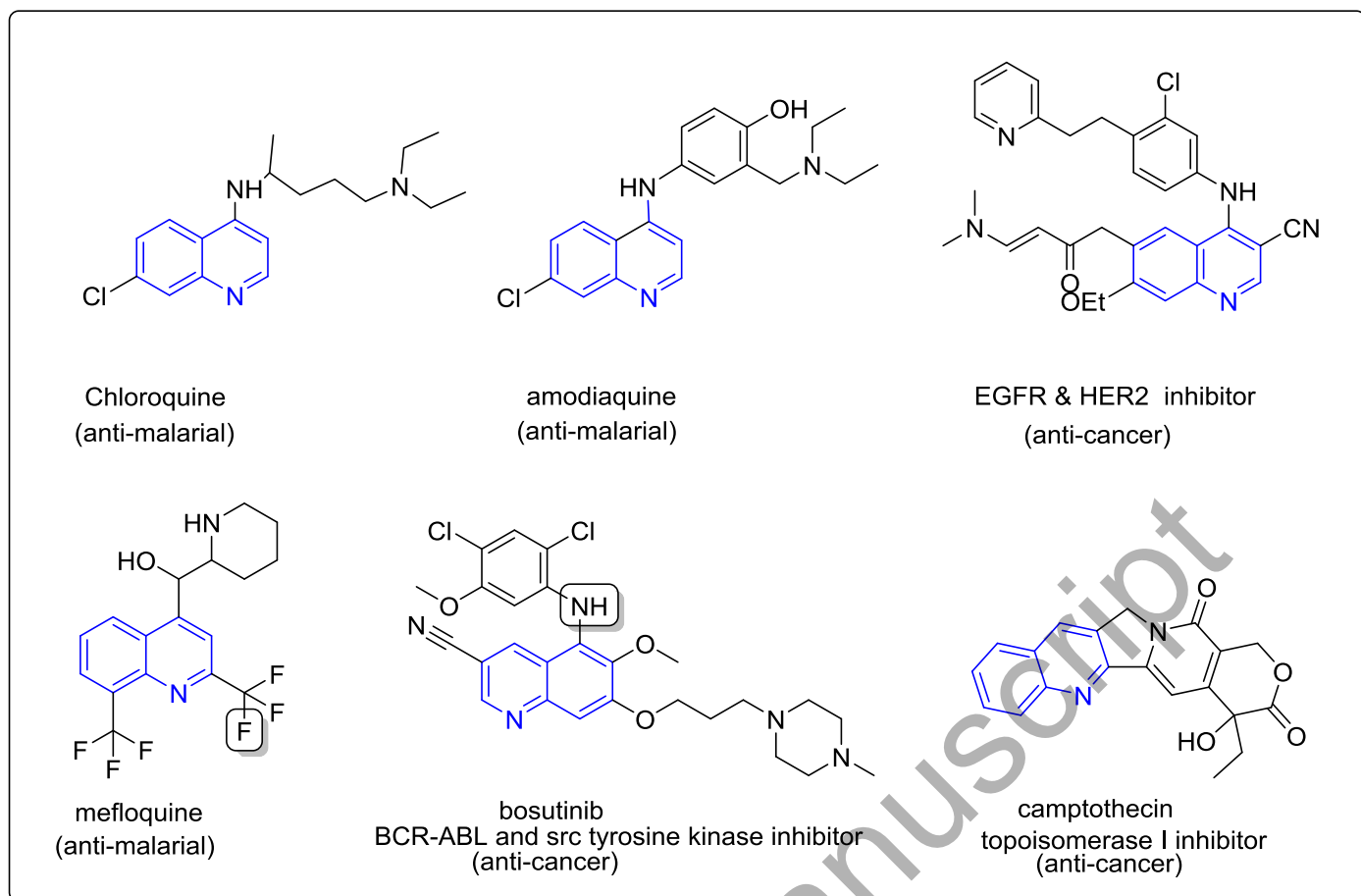


Figure 1. Important quinoline containing drugs

It is the main cargo and a delivery vehicle for transporting the drug molecules to their target organs and plays an unavoidable role in pharmacokinetic properties of drugs (Varshney et al., 2010). Also the conformational adaptability of serum albumin extends well beyond the immediate vicinity of the binding sites. Considering these facts, several literatures have been reported accounting the serum albumin interactions with the drug/drug like, herbicide, pesticide, dye compounds, biomolecules etc. (Bagoji et al, 2017, Roy et al., 2018; Salci & Toprak, 2017; Singh et al., 2017, Jafari et al., 2017). Hence it is important to address this factor to detail the ligand-binding properties (Fanali et al., 2012). In the current work, Human Serum Albumin (HSA) is selected as our protein model because of its wide range of functions involving the transport and

delivery of fatty acids, porphyrins, bilirubin, tryptophan, thyroxine, drug molecules and steroids. HSA consists of 585 amino acid residues and has more hydrophobic pockets inside the protein and is flexible to adapt its shape by means of altering its secondary or tertiary structure. HSA has three homologous domains (I, II and III) and each domain is divided into two subdomains (A and B). Drug binding to HSA takes place mostly at subdomain IIA and IIIA which are commonly referred to as Sudlow site I and II respectively (Ghuman et al., 2005). Molecular interactions at these sites can be monitored using intrinsic fluorescence properties of Trp214 (located in subdomain IIA). Some drug molecules, which are known as subdomain IIIA binders, can bind to subdomain IB to make it as a third major drug site (Zsila, 2013). Primary binding sites for fatty acids are located in subdomain IA and IIIA of HSA.

The binding nature of biologically potent quinoline scaffold with HSA is not known and the analysis may provide some important clues on its pharmacokinetics. In this aspect, the binding interactions between newly synthesized aminoquinolines and HSA were quantitatively analyzed based on spectroscopic characterizations such as UV-Vis, fluorescence, circular dichroism spectrometry and molecular modeling and the results are presented and discussed.

Materials and methods

Chemicals

All the chemicals used for the synthesis of compounds are of commercially available reagent grade (Merck, India). Commercially available human serum albumin was obtained from Sigma Aldrich, India and was used as received. Double distilled water was used throughout the work and the second distillation was carried out using alkaline permanganate. The stock solutions of HSA were prepared in an aqueous solution of Tris-HCL buffer (pH 7.4) and the compounds in 10% DMSO in buffer (v/v).

Instrumentation

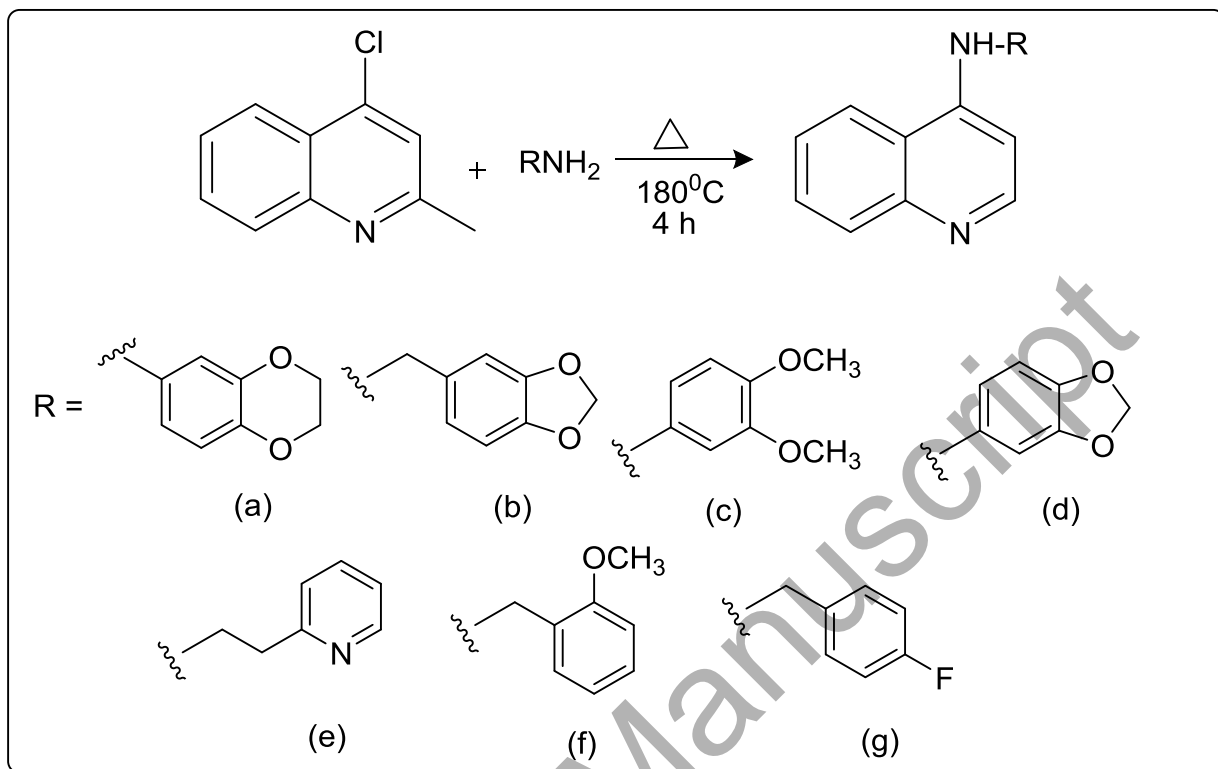
Nuclear magnetic resonance spectra were recorded in DMSO- d_6 (^1H NMR 300 MHz). The ^1H -NMR spectral data is expressed in the form: Chemical shift in units of ppm (normalized integration, multiplicity, and the value of J in Hz). Electro spray ion mass spectra (m/z) were recorded using LC/MSD TRAP XCT Plus (1200 Agilent). FT-IR spectra were recorded on a JASCO (FT-IR 460 Plus, Japan) spectrometer with samples prepared as KBr pellets. The absorption spectra were measured on a UV-Vis double beam spectrophotometer using 10 mm path length quartz cuvette (JASCO V630, Japan). Fluorescence measurements were performed with Cary Eclipse-Agilent Technologies spectrophotometer model G9800A equipped with xenon lamp using a 1.0-cm quartz cell. The excitation and emission slit width (5 nm) and the scan rate (250 nm) was kept constant for all of the experiments. Circular dichroism (CD) measurements were performed with a JASCO-810 spectrophotometer using a 1.0 mm path length quartz cell. Molecular docking studies were carried out using Maestro 11(Schrödinger LLC) installed in CentOS platform.

Procedures

General procedure for synthesis of compounds (1a-g)

To a stirred solution of 4-chloroquinoline, R-NH₂ (1eq) was slowly added at room temperature and the reaction mixture was stirred at 180°C for 4 h (Scheme 1). The completion of the reaction was monitored using thin layer chromatography (TLC). Once the reaction has been completed, the reaction mixture was cooled to RT and extracted with ethyl acetate. The combined organic layer was dried over anhydrous sodium sulfate and concentrated under reduced pressure. The reaction mixture was washed with hexane and ethyl acetate (10%) to get the pure product. The LC-MS and FT-IR spectra of all the compounds were given as Figure S1 and S2, respectively. The ^1H and ^{13}C

NMR spectral images for all the compounds were given as Figure S3 in supporting information.



Scheme 1. Synthesis of 4-substituted quinoline amines

N-(2,3-dihydrobenzo[*b*][1,4]dioxin-6-yl)-2-methylquinolin-4-amine (**1a**). Compound (**1a**) was prepared using the above mentioned procedure using 4-chloroquinoline (100 mg, 0.56 mmol) and 2,3-dihydrobenzo [b][1,4]dioxin-6-amine to obtain (**1a**) as white solid. M.p. 70-72°C. FTIR (KBr) cm^{-1} : 3406(N-H), 1203(C-O), 1065(C-N). ^1H NMR (DMSO- d_6 , 400 MHz, ppm): 8.672, s, 1H, 8.291-8.270 (d, $J=8.4\text{Hz}$, 1H), 7.762-7.742 (d, $J=8.0\text{Hz}$, 1H), 7.641-7.605(t, $J=7.2\text{Hz}$, 1H), 7.444-7.409 (t, $J=7.6,6.4\text{Hz}$, 1H), 6.930-6.908 (d, $J=8.8\text{Hz}$,1H) 6.835-6.812 (d, $J=9.2\text{Hz}$, 2H) 6.629,s,1H, 4.270,s,4H, 2.412,s,3H. ^{13}C NMR (DMSO- d_6 , 100 MHz, ppm): 159.06, 149.17, 148.91, 144.13, 140.77, 134.20, 129.57, 128.79, 124.09, 122.22, 118.45, 117.98, 117.35, 112.99, 101.0,

64.65, 64.45, 25.59. LCMS m/z: $[M+H]^+$ calculated for $C_{18}H_{16}N_2O_2$: 292.34, found: 293.5.

N-(benzo[d][1,3]dioxol-5-ylmethyl)-2-methylquinolin-4-amine (**1b**). Compound (**1b**) was prepared using the above mentioned procedure using 4-chloroquinaldine (50 mg, 0.28 mmol) and benzo[d][1,3]dioxol-5-ylmethanamine to obtain (**1b**) as white solid. M.p. 136-140°C. FTIR (KBr) cm^{-1} : 3433(N-H), 1251(C-O), 1038(C-N). 1H NMR (DMSO- d_6 , 400 MHz, ppm): 8.215-8.195 (d, $J=-8$ Hz, 1H), 7.698-7.676 (d, $J=8.8$ Hz, 2H), 7.568,s,1H, 7.385-7.369(d, $J=6.4$ Hz,1H), 6.960,s,1H, 6.869,s,1H, 6.292,s,1H, 5.974,s,2H, 4.438,s,2H, 2.380,s,1H. ^{13}C NMR (DMSO- d_6 , 100 MHz, ppm):158.98, 150.23, 148.55, 147.86, 146.57, 133.37, 129.15, 128.83, 123.64, 121.85, 120.50, 118.06, 108.58, 107.92, 101.30, 99.24, 45.74, 40.60, 39.35, 25.73. LCMS m/z: $[M+H]^+$ calculated for $C_{18}H_{16}N_2O_2$: 292.34, found: 293.5.

N-(3,4-dimethoxyphenyl)-2-methylquinolin-4-amine (**1c**). Compound (**1c**) was prepared using the above mentioned procedure using 4-chloroquinaldine (50 mg, 0.28 mmol) and 3,4-dimethoxy aniline to obtain (**1c**) as ash color solid. M.p. 90-94°C. FTIR (KBr) cm^{-1} : 3423(N-H), 1233 (C-O), 1025 (C-N). 1H NMR (DMSO- d_6 , 400 MHz, ppm): 8.767,s, 1H, 8.329-8.310 (d, $J= 7.6$ Hz, 1H), 7.772-7.751 (d, $J=8.4$ Hz, 1H), 7.654-7.617 (t, $J=7.2$ Hz,7.6Hz, 1H), 7.458-7.422 (t $J= 7.2$ Hz, 1H), 7.032-7.011(d, $J=8.4$ Hz, 1H), 6.950,s,1H, 6.905-6.885 (d, $J= 8$ Hz, 1H), 6.631,s,1H,3.788,s, 3H, 3.766,s,3H, 2.415,s,3H. ^{13}C NMR (DMSO- d_6 , 100 MHz, ppm): 159.14, 149.77, 149.35, 149.02,146.32, 133.89, 129.50, 128.99, 124.02, 122.18, 118.43, 116.28, 112.87, 109.23, 100.96, 56.19, 56.00, 40.59, 40.38, 40.18, 39.97, 39.76, 39.55, 39.34, 25.63. LCMS m/z: $[M+H]^+$ calculated for $C_{18}H_{18}N_2O_2$: 294.35, found: 295.6.

N-(benzo[d][1,3]dioxol-5-yl)-2-methylquinolin-4-amine (**1d**). Compound (**1d**) was prepared using the above mentioned procedure using 4-chloroquinaldine (50 mg, 0.28 mmol) and benzo[d][1,3]dioxol-5-amine to obtain (**1d**) as brown solid. M.p. 46°C. FTIR (KBr) cm^{-1} : 3416(N-H), 1233(C-O), 1025(C-N). ^1H NMR (DMSO- d_6 , 400 MHz, ppm): 8.707,s,1H, 8.296-8.276 (d,J=8Hz, 1H), 7.766-7.745 (d,J=8.4Hz, 1H), 7.644-7.607 (t, J=7.6Hz,7.2Hz, 1H), 7.448-7.412 (t, J=7.2Hz, 2H) 6.989-6.944 (t, J=8Hz,1H) 6.814-6.794(d, J=8Hz, 1H), 6.590,s,1H, 6.069,s,2H, 2.413,s,3H. ^{13}C NMR (DMSO- d_6 , 100MHz, ppm): 159.11, 149.36, 148.96, 148.32, 144.60, 134.92, 129.54, 128.85, 124.07, 122.20, 118.45, 117.49, 109.06, 106.15, 101.75, 101.11, 65.39, 25.61, 15.2. LCMS m/z: $[\text{M}+\text{H}]^+$ calculated for $\text{C}_{17}\text{H}_{14}\text{N}_2\text{O}_2$: 278.31, found: 279.5.

2-methyl-*N*-(pyridin-2-ylmethyl)quinolin-4-amine (**1e**). Compound (**1e**) was prepared using the above mentioned procedure using 4-chloroquinaldine (30 mg, 0.0168 mmol) and 2-(pyridin-2-yl)ethan-1-amine to obtain (**1e**) as light brown crystals. M.p. 110-116°C. FTIR (KBr) cm^{-1} : 3456(N-H). ^1H NMR (DMSO- d_6 , 400 MHz, ppm): 8.552-8.540 (d, J= 4.8Hz, 1H), 8.104-8.083 (d,J=8.4Hz, 1H), 7.735-7.672 (m, 2H), 7.566-7.528 (q, 1H), 7.363-7.315 (m, 2H), 7.256-7.226(q,1H), 7.173-7.147(t, J=5.2, 5.2Hz, 1H), 6.406,s,1H, 3.659-3.609 (q, 2H), 3.155-3.118 (t, J=7.6, 7.2Hz, 2H), 2.505-2.458 (d, J=18.8Hz, 3H). ^{13}C NMR (DMSO- d_6 , 100MHz, ppm): 159.55, 159.34, 150.50, 149.45, 148.01, 137.24, 129.41, 128.26, 123.96, 123.82, 122.20, 121.65, 117.79, 98.66, 42.71, 40.23, 40.02, 39.81, 39.60, 39.39, 39.18, 38.97, 36.63, 25.30. LCMS m/z: $[\text{M}+\text{H}]^+$ calculated for $\text{C}_{17}\text{H}_{17}\text{N}_3$: 263.35, found: 264.5.

N-(2-methoxybenzyl)-2-methylquinolin-4-amine (**1f**). Compound (**1f**) was prepared using the above mentioned procedure using 4-chloroquinaldine (50 mg, 0.28 mmol) and (2-methoxy phenyl) methanamine to obtain (**1f**) as pale pink solid. M.p. 170-172°C. FTIR (KBr) cm^{-1} : 3426(N-H). ^1H NMR (DMSO- d_6 , 400 MHz, ppm): 8.234-8.213 (d,

J= 8.4Hz, 1H), 7.707-7.688 (d,J=7.6Hz, 1H), 7.614-7.556 (q, 2H), 7.394-7.357 (q, 1H), 7.261-7.219 (m, 1H), 7.181-7.162 (d, J=7.6Hz, 1H),7.049-7.029 (d, J= 8Hz, 1H), 6.881-6.844 (t, J= 7.6, 7.2Hz, 1H), 6.194,s,1H, 4.490-4.476 (d, J= 5.6Hz, 2H), 3.888,s,3H, 2.360,s,3H. ^{13}C NMR (DMSO- d_6 , 100MHz, ppm): 159.04,157.28, 150.64,148.17, 129.40, 128.62, 128.46, 127.64, 126.28, 123.85,,121.79, 120.73, 117.86, 111.11, 98.86, 55.85, 40.91, 40.38, 40.17, 39.96, 39.75, 39.55, 39.34, 39.13, 25.44. LCMS m/z: $[\text{M}+\text{H}]^+$ calculated for $\text{C}_{18}\text{H}_{18}\text{N}_2\text{O}$: 278.36, found: 279.5.

N-(4-fluorobenzyl)-2-methylquinolin-4-amine (**1g**). Compound (**1g**) was prepared using the above mentioned procedure using 4-chloroquinaldine (50 mg, 0.28 mmol) and (4-fluorophenyl)methanamine to obtain (**1g**) as pale yellow solid. M.p. 70-74°C. FTIR (KBr) cm^{-1} : 3406(N-H). ^1H NMR (DMSO- d_6 , 400 MHz, ppm): 8.224-8.203 (d, J= 8.4Hz, 1H), 7.768-7.739 (t, J=6Hz, 1H), 7.702-7.681(d, J= 8.4Hz, 1H), 7.588-7.550 (q,1H), 7.445-7.355 (m, 3H), 7.178-7.133 (t, J= 9.2, 8.8Hz,1H), 6.271,s,1H, 4.534-4.519 (d, J= 6Hz,2H), 2.369,s,3H. ^{13}C NMR (DMSO- d_6 , 100MHz, ppm): 162.85, 160.44, 158.99, 150.44, 148.08, 135.47, 135.44, 129.45, 129.33, 129.25, 128.38, 123.92, 121.80, 117.92, 115.70, 115.49, 99.22, 45.20, 40.39, 40.18, 39.98, 39.77, 39.56, 39.35, 39.14, 25.36. LCMS m/z: $[\text{M}+\text{H}]^+$ calculated for $\text{C}_{17}\text{H}_{15}\text{FN}_2$: 266.32, found: 267.5.

Fluorescence measurements

A 2 mL solution containing 10 μM HSA was titrated by successive additions of compounds (**1a-g**) with concentrations ranging between 0 to 100 μM . These solutions were allowed to stand for a minute to equilibrate. The fluorescence emission spectra were then measured at room temperature with an excitation wavelength at 290 nm. The appropriate blank corresponding to the buffer solution was subtracted to correct for background fluorescence. The inner filter effect of the compounds on HSA quenching

has been corrected as reported (Suganthi & Elango, 2017). The binding constants of compounds (**1a-g**) to HSA were determined using the corrected emission intensity values.

UV-Vis absorption spectra

The UV-Vis absorption spectra of HSA in the absence and presence of aminoquinolines were measured over a wavelength range of 200-500 nm in the Tris-HCl buffer solution (pH 7.4) at room temperature.

CD studies

The CD spectra of HSA incubated with compounds (**1a-g**) at 1:1 molar ratio were recorded in the wavelength range of 200-500 nm under constant nitrogen flush using a 1.0 mm path length quartz cuvette. All observed spectra were baseline subtracted for buffer solution and the α -helical content was calculated on the basis of molar ellipticity value.

Molecular Docking

Structures of the compounds (**1a-g**) were sketched in using build panel and were prepared for docking using Ligprep module (Madhavy Sastry et al., 2013) implemented in Maestro 11 (Schrodinger LLC). The molecules were subjected to energy minimization with OPLS-2005 force field (Shivakumar et al., 2010) to generate single low energy 3-D structure for each input structure. For molecular docking studies, we utilized X-ray crystal structure of Human serum albumin and its three dimensional coordinates were obtained from Protein Data Bank (PDB ID: 5UJB). Protein was prepared by removal of solvent molecules coupled with the addition of hydrogen atoms using Prepwizard in Maestro. The missing side chains were built using prime and the active site was visually inspected and the appropriate corrections were made for tautomeric states of histidine residues, orientations of hydroxyl groups, and protonation

states of basic and acidic residues. The hydrogen atoms were minimized using OPLS2005 force field, while constraining all the heavy atoms (non-hydrogen) to their original positions. The protein with optimized hydrogen coordinates was finally saved as a separate file to be used for docking. For all the molecules, induced fit docking protocol implemented in Glide was used to carry-out the docking simulation.

In reality, HSA is one of the receptors which alter their binding site to conform to the shape and binding mode of the ligand which is reflected in CD experiment. This is often referred to as induced fit and is one of the main complicating factors in structure-based drug design. Hence, Induced Fit Docking (IFD) protocol which treats both the protein and ligand as flexible was used to generate new receptor conformations and ligand binding modes (Sherman et al., 2006, Karthikeyan et al., 2017).

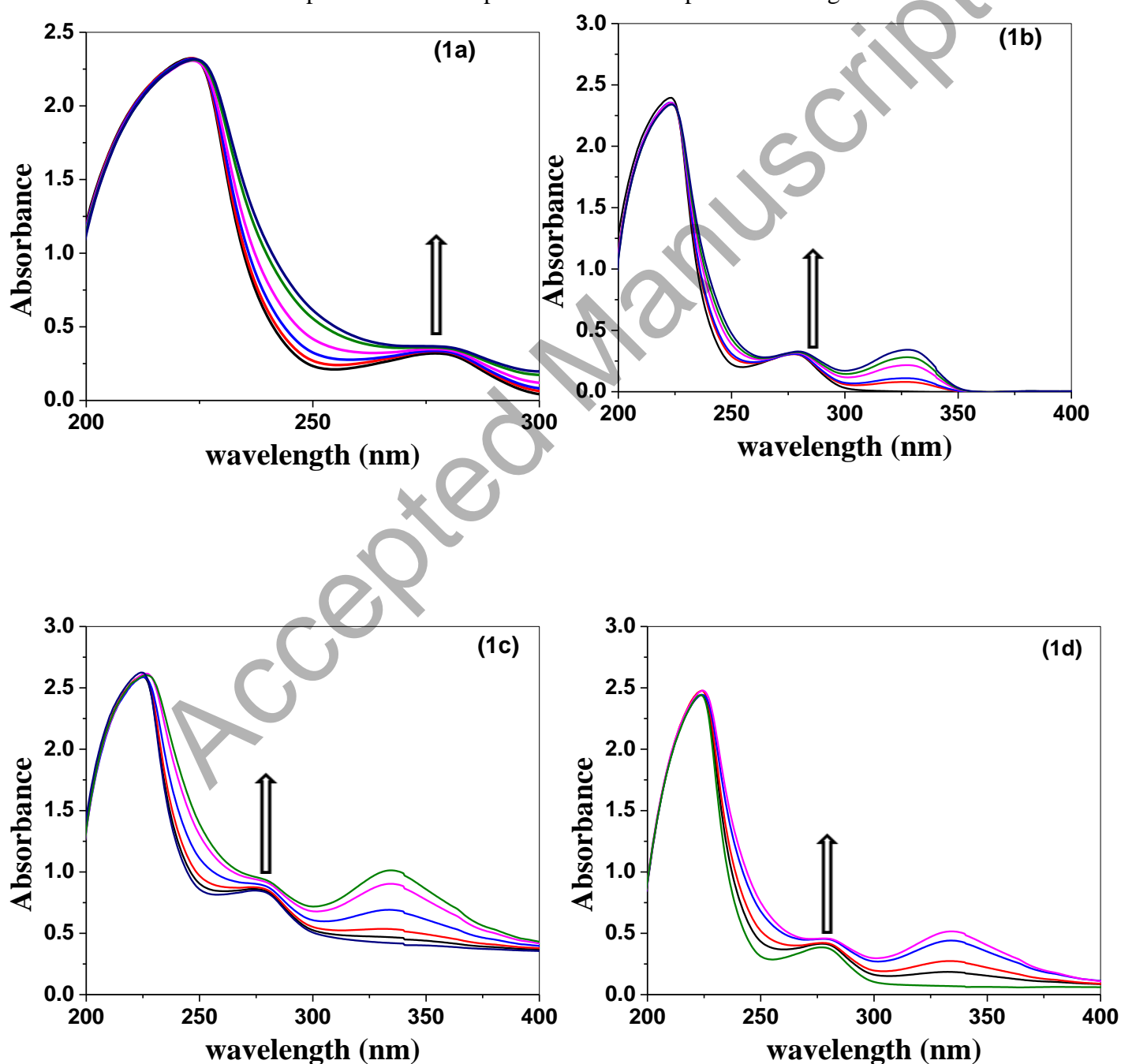
Results and Discussion

A series of 4-aminoquinoline derivatives were prepared and characterized by spectral techniques such as NMR, LC-MS and FTIR. These biologically important amino quinolines were tested for binding with transporter protein human serum albumin using UV-Vis, Fluorescence and CD spectrometry techniques. The binding site of the test compounds and their interactions with amino acid residues of HSA were revealed by molecular docking method and the results were discussed.

Absorption spectral studies

UV-Vis absorption spectroscopy is one of the effective methods in detecting the changes in the structural conformation of proteins upon binding to ligands. The absorption spectra of HSA in the absence and presence of increasing concentrations of the compounds are shown in Figure 2. The free HSA showed an absorption peak at 277 nm which is due to the polarity of the microenvironment around the tyrosine and tryptophan residues of HSA and other one at 223 nm due to the backbone of the protein.

Upon addition of the compounds the absorption intensity of the peak at 277 nm was found to increase with a small red-shift. This observation confirmed that all the compounds interacted with HSA and also changes the polarity of the microenvironment around the tyrosine and tryptophan residues of HSA and decreased the hydrophobicity of the binding site (Seedher & Agarwal, 2010). The quenching of protein backbone peak at 223 nm upon addition of the compounds suggested the quenching mechanism was mainly a static quenching process (Kumar et al., 2016). The results also indicated the formation of complex between the protein and the compounds in the ground state.



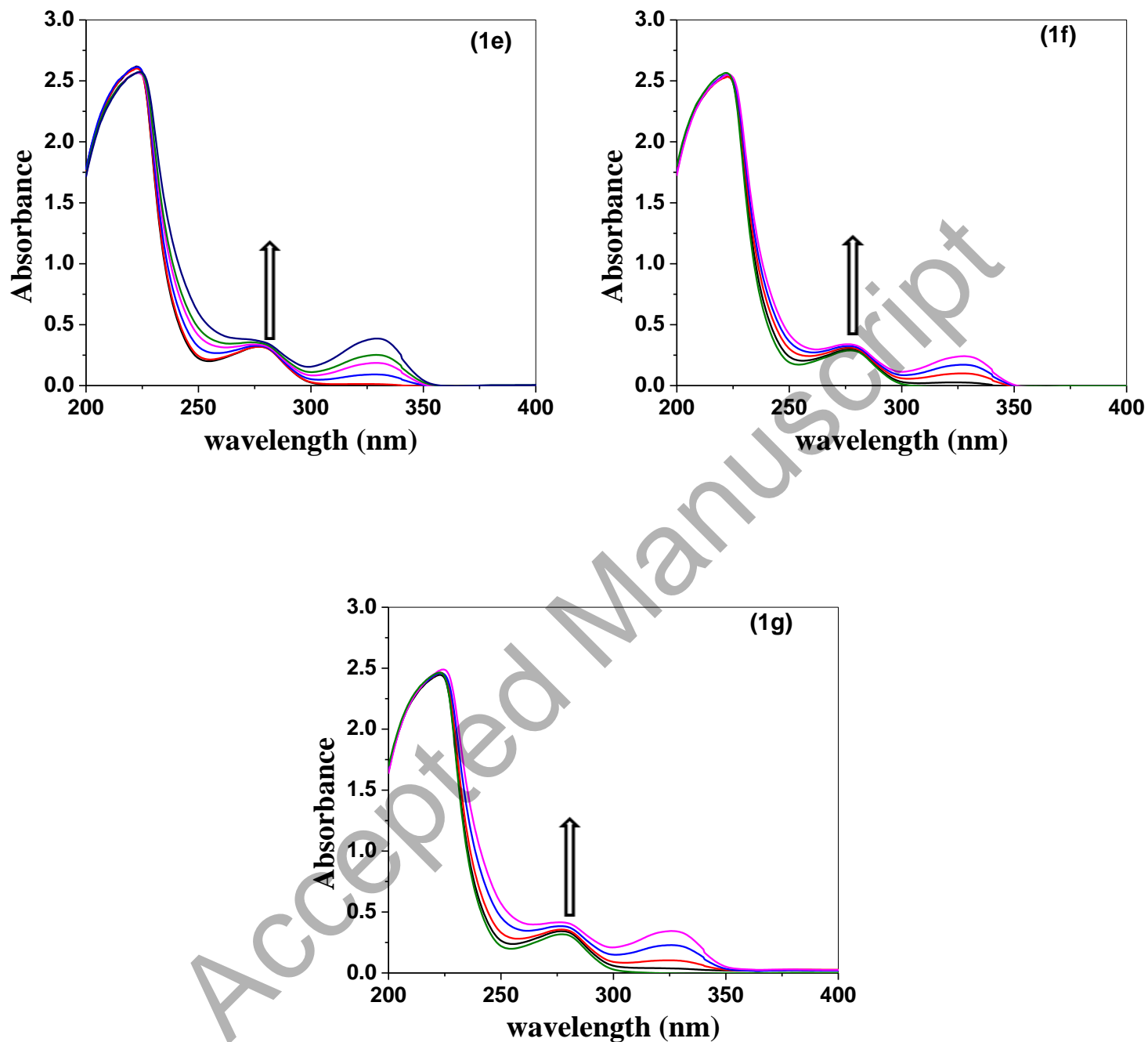


Figure 2. UV-Vis spectra of HSA- (**1a-g**) complex with increasing concentration from 0-50 μM with the Tris-HCl buffer solution (pH 7.4) at room temperature (298K)

Fluorescence quenching of HSA

The use of fluorescence spectroscopy to determine the quenching mechanism, mode and strength of interaction of HSA with drugs can be found in recently published reports, wherein the intrinsic fluorescent property of tryptophan is mainly utilized for the study (Zhou et al., 2018, Kosiha et al., 2017, Kosiha, Parthiban & Elango, 2017; Suganthi & Elango, 2017a; Suganthi & Elango, 2017b). When the HSA solution is excited at 290 nm, the maximum emission intensity of tryptophan will be contributed (Peng et al., 2016). In this study, the fluorescence spectra of HSA (10 μM) in the absence and presence of increasing concentrations (0 to 100 μM) of the compounds were recorded in Tris-HCl buffer solution (pH 7.4) at room temperature with excitation at 290 nm. Pure HSA exhibited a strong fluorescence emission at 348 nm (Figure 3). It is evident from the Figure 3 that with gradual increase in the concentration of these compounds, there is a significant reduction in the fluorescence emission intensity of HSA. A substantial red shift in the emission maximum (8-10 nm) was also observed suggesting that the polarity of the protein environment was higher in the protein-ligand complex when compared to pure HSA. The above observations indicated that there exists a significant binding of these compounds to HSA with changes in the microenvironment of tryptophan residues and conformation of protein structure.

In order to describe the quenching mechanism the fluorescence data is analyzed by Stern-Volmer equation.

$$F_0/F = 1 + K_{sv}[Q] \quad (1)$$

Where F_0 and F are the fluorescence intensities in the absence and presence of the quencher $[Q]$ and K_{sv} is the Stern-Volmer quenching constant which measures the efficiency of quenching (Khan et al., 2008). A plot of F_0/F versus $[Q]$, of all the compounds **1a-g**, are found to be linear (Figure 4) and the values of correlation

coefficient and K_{SV} are collected in Table 1. The linear Stern-Volmer plots indicated the occurrence of single type of quenching which may be static as per the absorption spectral confirmation.

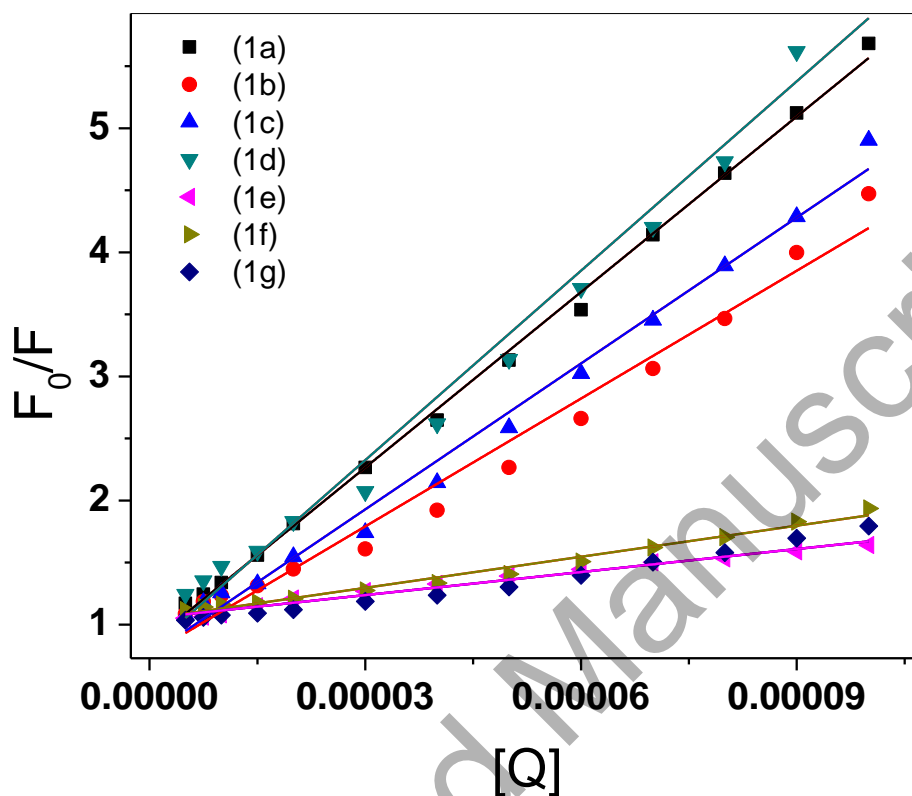


Figure 4. The Stern–Volmer plots of fluorescence titrations for compounds (**1a-g**) with HSA

To ascertain the mechanism of the quenching phenomena, as representative cases, the intrinsic fluorescence of HSA upon addition of **1a** and **1g** were measured at 298, 308 and 318 K and the thermodynamic parameters were calculated. The quenching constants for **1a** were found to be 4.72×10^4 , 6.21×10^4 and 5.30×10^4 L mol⁻¹ at 298, 308 and 318 K, respectively. For **1g**, K_{SV} values were found to be 1.22×10^4 , 3.05×10^4 and 2.41×10^4 L mol⁻¹ at 298, 308 and 318 K, respectively (Figure S4). These values don't

show any linear trend with increasing temperature. It is reported that, the static quenching constant doesn't necessarily decrease with an increase in temperature. Therefore, in the present study the quenching of fluorescence of HSA by these compounds occurs via static quenching mechanism (Hu, Liu, & Xiao, 2009; Tian et al., 2015).

Table 1. Stern-Volmer constant K_{sv} , correlation coefficient r and standard deviation **S.D** calculated from Stern-Volmer plot

Compounds	K_{sv} ($L mol^{-1}$)	r	S.D
1a	4.72×10^4	0.999	0.002
1b	3.90×10^4	0.990	0.001
1c	4.33×10^4	0.989	0.001
1d	5.76×10^4	0.993	0.003
1e	0.59×10^4	0.999	0.010
1f	0.91×10^4	0.998	0.006
1g	1.22×10^4	0.994	0.013

For a static quenching process, if it is assumed that there are similar and independent binding sites in the protein molecules, the binding constant (K_a) and number of binding sites (n) can be calculated from the following equation.

$$\log[(F_0 - F)/F] = \log K_a + n \log [Q] \quad (2)$$

where F_0 and F are the fluorescence intensity of HSA in the absence and presence of the ligands, respectively. The values of correlation coefficient and binding constants thus calculated are given in Table 2. The number of binding sites n was found nearly equal to 1, indicating that there was only one binding site in HSA for the compounds during their binding process and also indicates in the binding reaction, the molar ratio of HSA and the compounds is 1:1. The magnitude of the binding constant values in the order of 10^4 - 10^5 M^{-1} obtained suggested that there is a significant interaction between the compounds and the protein molecule. As representative cases, the binding constants for the interaction of **1a** and **1g** with HSA were also calculated at three different temperatures. The K_a values obtained are 13.80×10^4 , 9.46×10^4 and 4.99×10^4 (for **1a**) and 2.20×10^3 , 0.98×10^3 and 0.65×10^3 (for **1g**) at 298, 308 and 318 K, respectively. From these binding constant values, the thermodynamic parameters were evaluated using van't Hoff equation ($\ln K_a = -\Delta H/RT + \Delta S/R$, where K_a is the binding constant, R is the gas constant and T is the temperature). For both these systems plot of $\ln K_a$ versus $1/T$ was found to be linear (Figure S5). The enthalpy, entropy and free energy changes obtained are: For **1a**, $\Delta H = -44$ kJ mol^{-1} ; $\Delta S = -48$ J mol^{-1} and $\Delta G = -58$ kJ mol^{-1} ; For **1g**, $\Delta H = -48$ kJ mol^{-1} ; $\Delta S = -98$ J mol^{-1} and $\Delta G = -77$ kJ mol^{-1} . The observed $\Delta H < 0$ and $\Delta S < 0$ indicated that the main forces acting between HSA and these compounds are hydrogen bonds and van der Waals forces and the interaction reactions were exothermic (Ross & Subramanian, 1981). The negative Gibbs free energy changes indicated that the interaction of these compounds with HSA is spontaneous.

Table 2. Association constant K_a , number of binding site n , Correlation coefficient r , standard deviation **S.D** calculated from $\log((F_0 - F)/F)$ versus $\log [Q]$

Compounds	K_a ($L mol^{-1}$)	n	r	S.D
1a	1.38×10^5	1.118	0.999	0.0010
1b	4.731×10^4	1.032	0.997	0.0102
1c	0.907×10^5	1.118	0.997	0.0023
1d	1.05×10^5	1.084	0.999	0.0011
1e	0.138×10^4	0.59	0.989	0.0022
1f	0.118×10^4	0.786	0.991	0.0111
1g	0.22×10^4	0.83	0.994	0.0023

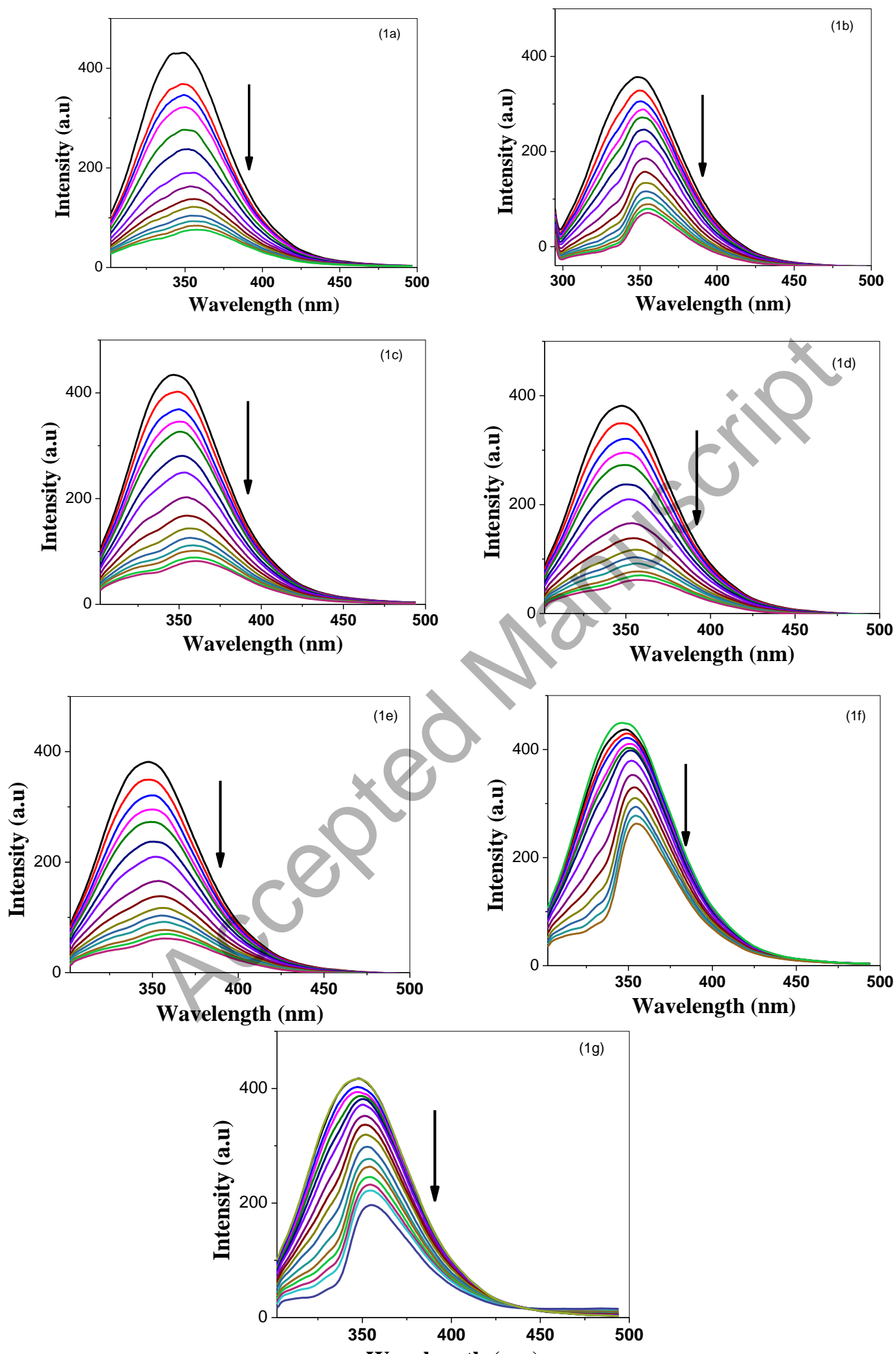


Figure 3. Fluorescence emission quenching of HSA (10 μM) upon addition of compounds (**1a-g**) complex with increasing concentration from 0-100 μM in the Tris-HCl buffer solution (pH 7.4) at room temperature (298 K)

Binding distance between HSA and 1a-g

The binding distance between the receptor and the ligands is related to the critical energy transfer distance as given in Förster non-radiation energy transfer theory (Suganthi & Elango, 2017). It is given by the equation

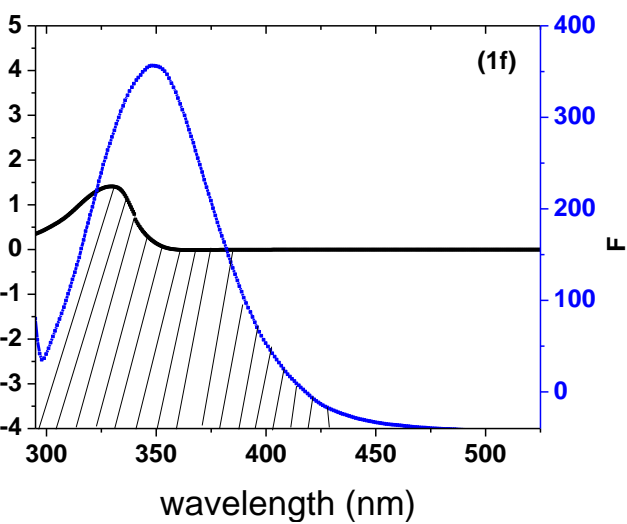
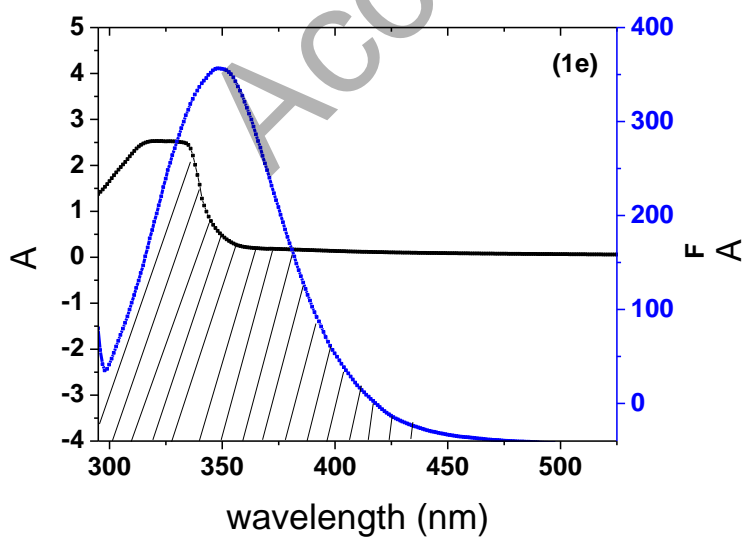
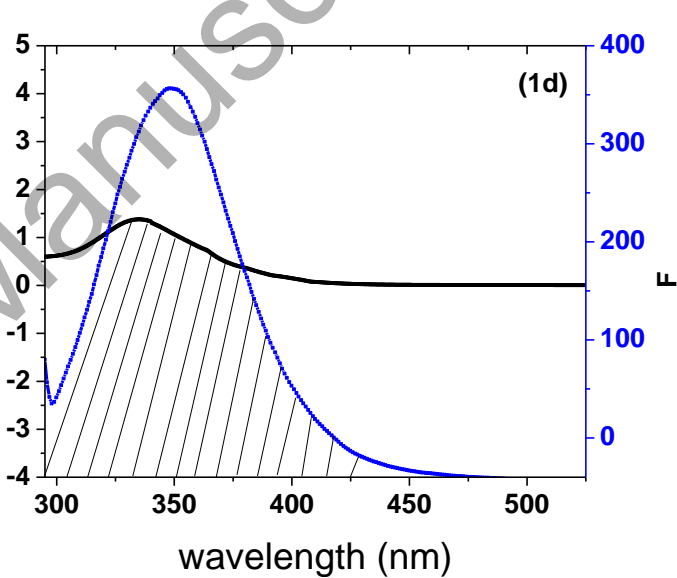
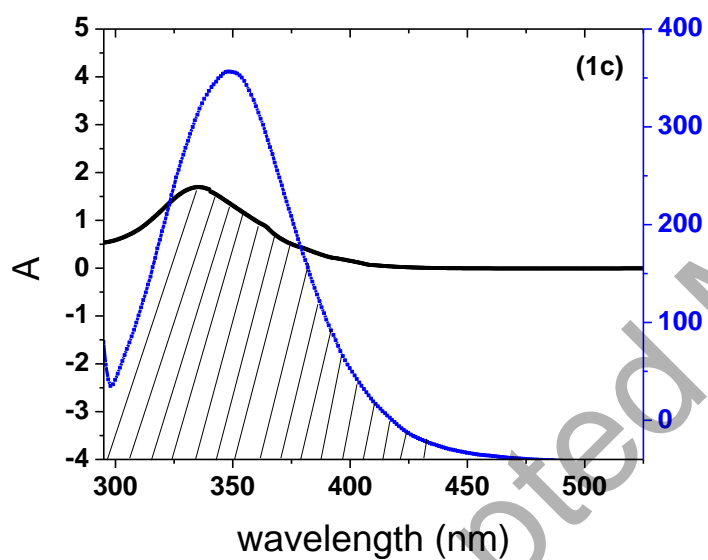
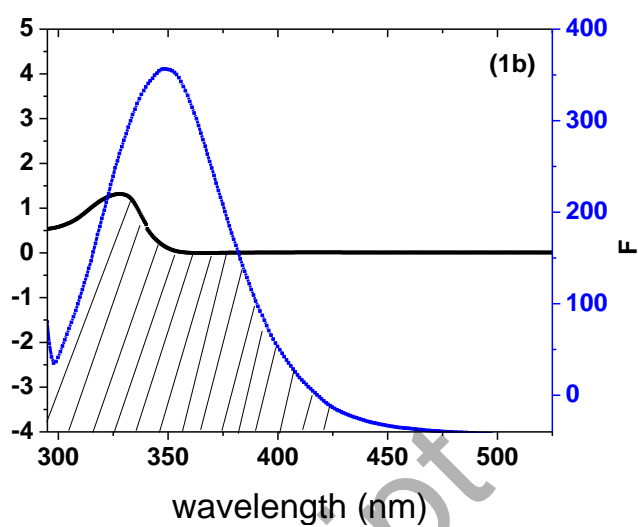
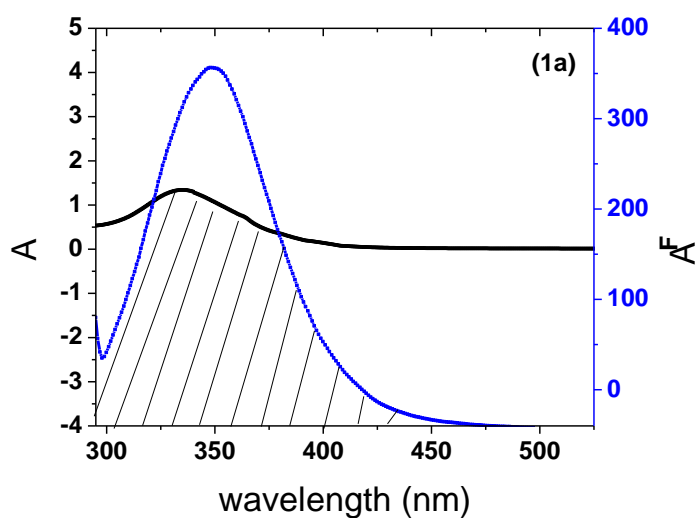
$$E = R_0^6 / (R_0^6 + r^6) = 1 - (F/F_0) \quad (3)$$

Where E is the energy transfer efficiency, R_0 is the critical distance when the energy transfer efficiency is 50%, and r is the binding distance between donor and acceptor.

Also

$$R_0^6 = 0.2108 [N^{-4} \times \varphi_d \times K^2 \times J], \quad (4)$$

Where K^2 is the spatial orientation factor of the dipole, N is the refractive index of the medium, φ_d is the fluorescence quantum yield of the donor, and J is the overlap integral of the fluorescence emission spectrum of the donor and the absorption spectrum of the acceptor. The overlap of the absorption spectra of the test compounds and the emission spectra of HSA is shown in Figure 5. The spectrum overlap integral is calculated using fluortools (UV-Vis-IR spectral analysis software) with $N = 1.336$, $\varphi_d = 0.15$, $K^2 = 2/3$ and R_0 and r values calculated are collected in Table 3. All the calculated r values are less than 8 nm indicating the highest possibility of energy transfer between HSA and the test compounds.



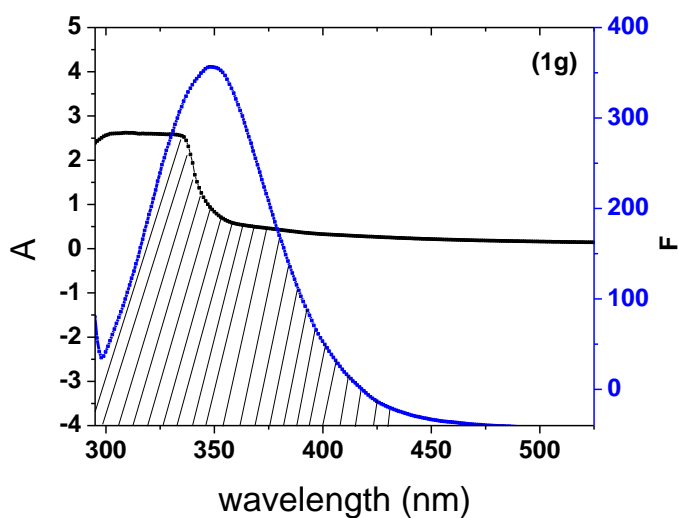


Figure 5. Spectral overlap of absorption and emission from test compounds and HSA, respectively

Table 3. Donor-acceptor distance r between HSA and the compounds calculated using FRET theory

Compounds	J ($\text{cm}^3 \text{L M}^{-1}$)	E (%)	R_0 (nm)	r (nm)
1a	1.386×10^{10}	0.17	0.853	1.10
1b	5.603×10^9	0.08	0.724	1.09
1c	1.707×10^{10}	0.07	0.872	1.34
1d	1.415×10^{10}	0.09	0.845	1.26
1e	6.173×10^9	0.05	0.736	1.19
1f	1.434×10^{10}	0.027	0.847	1.54
1g	1.845×10^{10}	0.034	0.883	1.55

Circular dichroism studies

The structural change of HSA by the binding of ligands can be determined by CD measurements. CD spectra of pure HSA and that after the addition of the compounds (**1a-g**) are given in Figure 6. The CD spectrum of pure HSA has two negative peaks at 209 and 222 nm, which correspond to α -helical structure of the protein owing to $\pi \rightarrow \pi^*$ and $n \rightarrow \pi^*$ transitions in the peptide bond in helices, respectively (Wang et al., 2008). Changes in the ellipticity at 209 and 222 nm by the addition of compounds are useful probes for visualizing changes in the protein's α -helical structure (Na Ji et al., 2015). The CD results are usually expressed as mean residue ellipticity (MRE) with $\text{deg cm}^2 \text{ dmol}^{-1}$ as units according to the following equation (Berova et al. 2000).

$$MRE = \frac{\text{Observed CD (m deg)}}{C_p \times n \times l \times 10} \quad (5)$$

where C_p is the molar concentration of the protein, n is the number of amino acid residues and l is the path length. The α -helicity of free and combined HSA were calculated from MRE values using the following equation

$$\alpha - \text{helix (\%)} = \left\{ \frac{-MRE_{222} - 2340}{30300} \right\} \times 100 \quad (6)$$

where MRE_{222} is the observed MRE value at 222 nm. In this experiment, $C_p = 1 \mu\text{M}$, n is 585, l is 1.0 mm. With the above equations and experimental data, the α -helix % were calculated and given in Table 4.

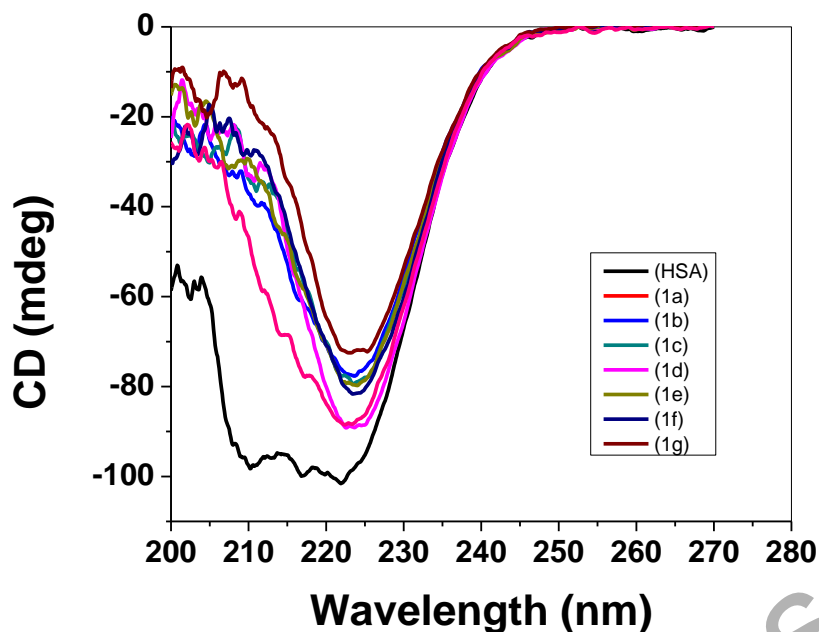


Figure 6. CD spectra in the absence and presence of test compounds with HSA (10 μ M) at 1:1 ratio concentration

It was suggested that the formation of HSA-ligands complex perturbs the secondary structural elements of HSA where the ligands bound with the amino acid residues of the main poly peptide chain, which confirms the interaction of the ligands with protein. Also, the observation of minor increase in ellipticity (~ 30 Mdeg) at 222 nm indicated that the protein structure remains predominantly helix and decrease in α -helicity suggested that there were slight perturbations in the conformation of α -helices of the protein during binding of these compounds (Wei et al., 2014).

Table 4. Change in helical percentage in HSA upon addition of compounds calculated using the absorbance value from CD spectrum at 222 nm.

System	<i>Observed CD (m deg)</i>	α – <i>helix (%)</i>
Free HSA	-101.466	49
HSA + 1a	-88.1414	42
HSA + 1b	-69.4206	31
HSA + 1c	-76.1836	35
HSA + 1d	-77.6536	36
HSA + 1e	-78.7693	37.
HSA + 1f	-79.0823	37
HSA + 1g	-71.8374	33

Binding site prediction

The induced fit docking studies of HSA with test compounds were carried out initially to validate the docking algorithm. In this study, both the protein and the compounds are treated flexible so as to predict the binding site exactly with the conformational changes of HSA. All the test compound structures were prepared by ligand preparation wizard and the protein was refined by protein preparation wizard by adding the missing side chains and removal of waters. Also, the cocrystallized ligand propofol in PDB structure 5UJB was redocked to HSA by setting the grid box length equal to 40Å in order to test the ability of the program to redetermine the docking site as site III in HSA which was originally observed in HSA-propofol crystallized complex.

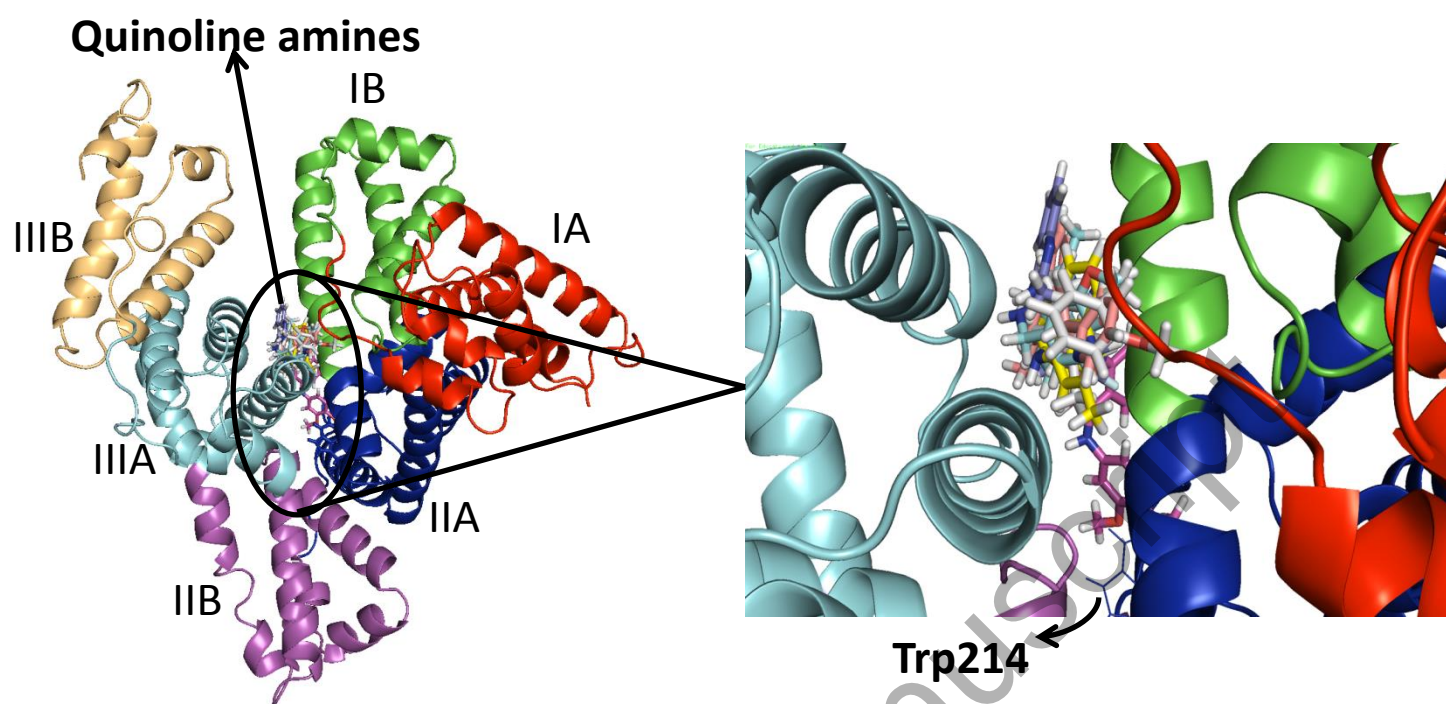


Figure 9. Binding site of all the synthesized quinoline amines in HSA.

Accepted Manuscript

Table 5. IFD results showing the highly scored pose of the docked orientation of the test compounds and the bonded amino acid residues in the binding site.

Compounds	ΔG_{exp} (kcal/mol)	Docking score		Interacting residues
		ΔG_{calc} (kcal/mol)	Glide energy (kcal/mol)	
1a	-7.003	-8.063	-61.189	Lys432, Asp451, Arg218
1b	-6.370	-6.693	-57.479	Arg197
1c	-6.755	-7.727	-58.113	Tyr 452
1d	-6.842	-8.419	-38.585	Tyr452, Val455
1e	-4.265	-7.733	-48.173	Trp214, Arg218
1f	-4.185	-7.724	-58.450	Lys190
1g	-4.554	-7.089	-53.588	Tyr452, Lys432

$\Delta G_{\text{exp}} = -RT \ln K_a$

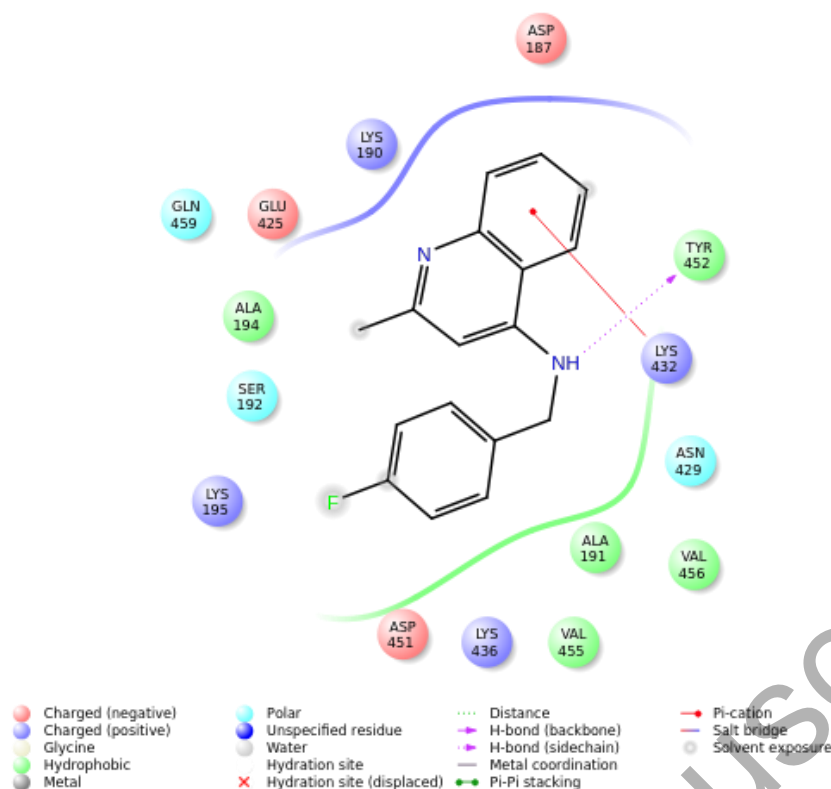


Figure 8. Ligands + Binding sites created from Maestro depicting the type of interactions with HSA

As expected the docking energy (-76.975 kcal/mol) and the docking score (-12.168 kcal/mol) was found to be higher and at the same time, the RMSD value between the crystal structure complex and the redocked complex was found 0.209 which indicated the parameter settings and the program ability to determine the binding site is fine. The binding site was correctly located and the interactions between propofol and HSA were similar as in crystal structure. Hence the same procedure was followed for the docking of the compounds under investigation and the results obtained are tabulated in Table 5. The negative docking score and glide energy indicated the binding of these compounds with HSA. All the seven compounds were found to be docked in the cleft formed by the interface of the domains IIA and IIIA (Figure 7). This is referred as the Iodipamide (a radiopaque drug used to diagnose certain medical problems) binding site which was

explained in the X-ray co-crystal complex with PDB Id: 2BXN. While the drug sites 1 (domain IIA) and 2 (domain IIIA) were found to be highly adaptable and some other clefts are utilized by local ligand induced conformational changes in the protein and revealed secondary binding sites (Ghuman et al., 2005). This docking study provided the consistent result of binding of these compounds with one such secondary binding site which overlapped the endogenous ligand tyroxine site 5. As seen in Figure 8, the binding cavity wall was enveloped with hydrophobic residues and with few positively charged residues. It was also observed that all the compounds (**1a-g**) interacted with Tyr452 either by π - π interaction or by means of hydrogen bond or by hydrophobic interaction. Also **1a** and **1c** possessed hydrophobic contact with Trp214 and **1e** had π - π interaction between the aromatic rings. The conformational changes in both protein and ligand in this docking study revealed that the particular type of ligand orientations in the binding cleft of HSA might have been contributed to fluorescence quenching in Tyr/Trp. These factors also substantiated the slightly varied well defined quenching of **1a**, **1c** and **1e** when compared to other four compounds in the fluorescence experiments. The slight variation in the Gibbs free energy changes associated with the docking scores might be attributed to omission of solvent in docking calculations. Also, this study provides valuable insights into quinoline amines-HSA interactions and facilitates the efforts to modify new quinoline lead compounds to control their interaction with HSA and to optimize their distribution in human body.

Conclusions

A series of new 4-substituted quinoline amine derivatives were synthesized and characterized. Their binding with human serum albumin was investigated using multiple spectroscopic techniques. The quenching of the $n \rightarrow \pi^*$ peak in UV-Vis spectrum indicated the HSA-ligand complex formation. Fluorescence quenching at 277 nm and

the binding constants in the order of 10^4 M^{-1} proved the better binding of the compounds as compared to many reported drugs. The quenching mechanism was found to be static overall and the binding reaction is exothermic and spontaneous. The hydrogen bonds and van der Waals forces were found to be dominant in HSA interaction with these compounds. The binding distance calculated using the FRET theory was found to be less than 2 nm for all the compounds with HSA indicating the highest possibility of complex formation. The slight decrease in the helical structure percentage derived from CD spectra confirmed the changes in the protein conformation of HSA upon binding with these compounds. The induced fit molecular docking study revealed the iodipamide binding site as the site of binding for these quinoline amines in HSA molecule. These compounds interact with Trp-214 and Tyr 452 by hydrogen bonds and van der Waals forces.

Acknowledgement

The authors are highly thankful to the Department of Science and Technology, New Delhi for financial support under WOS-A Scheme (SR/WOS-A/CS-1084/2014). KNV acknowledges the computational facility and Schrodinger access offered by Prof. D. Velmurugan, BSR Faculty, Center for crystallography and Biophysics, University of Madras, Chennai.

References

- Afzal, O., Kumar, S., Ali, R., Kumar, R., Jaggi, M., & Bawa, S. (2015). European Journal of Medicinal Chemistry Review article A review on anticancer potential of bioactive heterocycle quinoline, 97. <https://doi.org/10.1016/j.ejmech.2014.07.044>
- Bagoji, A. M., Gowda, J. I., Gokavi, N. M., & Nandibewoor, S. T. (2017). Multi-spectroscopic and voltammetric evidences for binding, conformational changes of

- bovine serum albumin with thiamine. *Journal of Biomolecular Structure and Dynamics*, 35(11), 2395–2406. <https://doi.org/10.1080/07391102.2016.1220332>
- Chan, S. H., Chui, C. H., Chan, S. W., Kok, S. H. L., Chan, D., Tsoi, M. Y. T., Tang, J. C. O. (2012). Synthesis of 8-Hydroxyquinoline Derivatives as Novel Antitumor Agents.
- Eswaran, S., Adhikari, A. V., Chowdhury, I. H., Pal, N. K., & Thomas, K. D. (2010). New quinoline derivatives: Synthesis and investigation of antibacterial and antituberculosis properties. *European Journal of Medicinal Chemistry*, 45(8), 3374–3383. <https://doi.org/10.1016/j.ejmech.2010.04.022>
- Fanali, G., Di Masi, A., Trezza, V., Marino, M., Fasano, M., & Ascenzi, P. (2012). Human serum albumin: From bench to bedside. *Molecular Aspects of Medicine*, 33(3), 209–290. <https://doi.org/10.1016/j.mam.2011.12.002>
- Ghuman, J., Zunszain, P. A., Petitpas, I., Bhattacharya, A. A., Otagiri, M., & Curry, S. (2005). Structural basis of the drug-binding specificity of human serum albumin. *Journal of Molecular Biology*, 353(1), 38–52. <https://doi.org/10.1016/j.jmb.2005.07.075>
- Hayat, F., Moseley, E., Salahuddin, A., Van Zyl, R. L., & Azam, A. (2011). Antiprotozoal activity of chloroquinoline based chalcones. *European Journal of Medicinal Chemistry*, 46(5), 1897–1905. <https://doi.org/10.1016/j.ejmech.2011.02.004>
- Heidary, D. K., Howerton, B. S., & Glazer, E. C. (2014). Coordination of hydroxyquinolines to a ruthenium bis-dimethyl-phenanthroline scaffold radically improves potency for potential as antineoplastic agents. *Journal of Medicinal Chemistry*, 57(21), 8936–8946. <https://doi.org/10.1021/jm501043s>
- Hu, Y.-J., Liu, Y., & Xiao, X.-H. (2009). Investigation of the interaction between

Berberine and human serum albumin. *Biomacromolecules*, 10(3), 517–521.

<https://doi.org/10.1021/bm801120k>

Jafari, F., Samadi, S., Nowroozi, A., Sadrjavadi, K., Moradi, S., Ashrafi-Kooshk, M. R.,

& Shahlaei, M. (2017). Experimental and computational studies on the binding of

diazinon to human serum albumin. *Journal of Biomolecular Structure and*

Dynamics, 1102(May), 1–21. <https://doi.org/10.1080/07391102.2017.1329096>

Jain, S., Chandra, V., Kumar, P., Pathak, K., Pathak, D., & Vaidya, A. (2016).

Comprehensive review on current developments of quinoline-based anticancer

agents. *Arabian Journal of Chemistry*. <https://doi.org/10.1016/j.arabjc.2016.10.009>

Karthikeyan, S., Bharanidharan, G., Mani, K. A., Srinivasan, N., Keshewani, M.,

Velmurugan, D., Ganesan, S. (2017). Determination on the binding of thiadiazole

derivative to human serum albumin: a spectroscopy and computational approach.

Journal of Biomolecular Structure and Dynamics, 35(4), 817–828.

<https://doi.org/10.1080/07391102.2016.1162751>

Khan, S. N., Islam, B., Yennamalli, R., Sultan, A., Subbarao, N., & Khan, A. U. (2008).

Interaction of mitoxantrone with human serum albumin: Spectroscopic and

molecular modeling studies. *European Journal of Pharmaceutical Sciences*, 35(5),

371–382. <https://doi.org/10.1016/j.ejps.2008.07.010>

Korotchenko, V., Sathunuru, R., Gerena, L., Caridha, D., Li, Q., Kreishman-Deitrick,

M., ... Lin, A. J. (2015). Antimalarial activity of 4-amidinoquinoline and 10-

amidinobenzonaphthyridine derivatives. *Journal of Medicinal Chemistry*, 58(8),

3411–3431. <https://doi.org/10.1021/jm501809x>

Kosiha, A., Parthiban, C., Ciattini, S., Chelazzi, L., & Elango, K. P. (2017). Metal

complexes of naphthoquinone based ligand: synthesis, characterization, protein

binding, DNA binding/cleavage and cytotoxicity studies. *Journal of Biomolecular*

Structure and Dynamics, 1102(December), 1–12.

<https://doi.org/10.1080/07391102.2017.1413423>

Kosiha, A., Parthiban, C., & Elango, K. P. (2017). Synthesis, characterization and DNA binding/cleavage, protein binding and cytotoxicity studies of Co(II), Ni(II), Cu(II) and Zn(II) complexes of aminonaphthoquinone. *Journal of Photochemistry and Photobiology B: Biology*, 168, 165–174.

<https://doi.org/10.1016/j.jphotobiol.2017.02.010>

Kumar, A., Kumar, A., Gupta, R. K., Paitandi, R. P., Singh, K. B., Trigun, S. K., ... Pandey, D. S. (2016). Cationic Ru(II), Rh(III) and Ir(III) complexes containing cyclic π -perimeter and 2-aminophenyl benzimidazole ligands: Synthesis, molecular structure, DNA and protein binding, cytotoxicity and anticancer activity. *Journal of Organometallic Chemistry*, 801, 68–79.

<https://doi.org/10.1016/j.jorganchem.2015.10.008>

Kumar, S., Bawa, S., & Gupta, H. (2009). Biological Activities of Quinoline Derivatives Biological Activities of Quinoline Derivatives, (December).

<https://doi.org/10.2174/138955709791012247>

Lilienkampf, A., Jialin, M., Baojie, W., Yuehong, W., Franzblau, S. G., & Kozikowski, A. P. (2009). Structure-Activity relationships for a series of quinoline-based compounds active against replicating and nonreplicating mycobacterium tuberculosis. *Journal of Medicinal Chemistry*, 52(7), 2109–2118.

<https://doi.org/10.1021/jm900003c>

Madhavi Sastry, G., Adzhigirey, M., Day, T., Annabhimoju, R., & Sherman, W. (2013). Protein and ligand preparation: Parameters, protocols, and influence on virtual screening enrichments. *Journal of Computer-Aided Molecular Design*, 27(3), 221–

234. <https://doi.org/10.1007/s10822-013-9644-8>

- Musiol, R., Jampilek, J., Buchta, V., Silva, L., Niedbala, H., Podeszwa, B., ... Polanski, J. (2006). Antifungal properties of new series of quinoline derivatives. *Bioorganic & Medicinal Chemistry*, *14*(10), 3592–3598.
<https://doi.org/10.1016/j.bmc.2006.01.016>
- Oliva, A., Meepagala, K. M., Wedge, D. E., Harries, D., Hale, A. L., Aliotta, G., & Duke, S. O. (2003). Natural fungicides from *Ruta graveolens* L. leaves, including a new quinolone alkaloid. *Journal of Agricultural and Food Chemistry*, *51*(4), 890–896. <https://doi.org/10.1021/jf0259361>
- Peng, X., Wang, X., Qi, W., Su, R., & He, Z. (2016). Affinity of rosmarinic acid to human serum albumin and its effect on protein conformation stability. *Food Chemistry*, *192*, 178–187. <https://doi.org/10.1016/j.foodchem.2015.06.109>
- Ross, P. D., & Subramanian, S. (1981). Thermodynamics of Protein Association Reactions: Forces Contributing to Stability. *Biochemistry*, *20*(11), 3096–3102. <https://doi.org/10.1021/bi00514a017>
- Roy, A., Seal, P., Sikdar, J., Banerjee, S., & Haldar, R. (2018). Underlying molecular interaction of bovine serum albumin and linezolid: a biophysical outlook. *Journal of Biomolecular Structure and Dynamics*, *36*(2), 387–397. <https://doi.org/10.1080/07391102.2017.1278721>
- Salci, A., & Toprak, M. (2017). Spectroscopic investigations on the binding of Pyronin Y to human serum albumin. *Journal of Biomolecular Structure and Dynamics*, *35*(1), 8–16. <https://doi.org/10.1080/07391102.2015.1128357>
- Seedher, N., & Agarwal, P. (2010). Complexation of fluoroquinolone antibiotics with human serum albumin: A fluorescence quenching study. *Journal of Luminescence*, *130*(10), 1841–1848. <https://doi.org/10.1016/j.jlumin.2010.04.020>
- Sherman, W., Day, T., Jacobson, M. P., Friesner, R. A., & Farid, R. (2006). Novel

- Procedure for Moldeing Ligand/Receptor Induced Fit Effects. *J Med Chem*, 49(2), 534–553. <https://doi.org/10.1021/jm050540c>
- Shivakumar, D., Williams, J., Wu, Y., Damm, W., Shelley, J., & Sherman, W. (2010). Prediction of Absolute Solvation Free Energies using Molecular Dynamics Free Energy Perturbation and the OPLS Force Field. *J Chem Theory Comput*, 6(5), 1509–1519. <https://doi.org/10.1021/ct900587b>
- Singh, N., Pagariya, D., Jain, S., Naik, S., & Kishore, N. (2017). Interaction of copper (II) complexes by bovine serum albumin: spectroscopic and calorimetric insights. *Journal of Biomolecular Structure and Dynamics*, 1102(July), 1–14. <https://doi.org/10.1080/07391102.2017.1355848>
- Suganthi, M., & Elango, K. P. (2017). Binding of organophosphate insecticides with serum albumin: multispectroscopic and molecular modelling investigations. *Physics and Chemistry of Liquids*, 55(2), 165–178. <https://doi.org/10.1080/00319104.2016.1183006>
- Suganthi, M., & Elango, K. P. (2017). Synthesis, characterization and serum albumin binding studies of vitamin K3 derivatives. *Journal of Photochemistry and Photobiology B: Biology*, 166, 126–135. <https://doi.org/10.1016/j.jphotobiol.2016.11.016>
- Thomas, K. D., Adhikari, A. V., Telkar, S., Chowdhury, I. H., Mahmood, R., Pal, N. K., ... Sumesh, E. (2011). Design, synthesis and docking studies of new quinoline-3-carbohydrazide derivatives as antitubercular agents. *European Journal of Medicinal Chemistry*, 46(11), 5283–5292. <https://doi.org/10.1016/j.ejmech.2011.07.033>
- Tian, Z., Zang, F., Luo, W., Zhao, Z., Wang, Y., Xu, X., & Wang, C. (2015). Spectroscopic study on the interaction between mononaphthalimide spermidine

- (MINS) and bovine serum albumin (BSA). *Journal of Photochemistry and Photobiology B: Biology*. <https://doi.org/10.1016/j.jphotobiol.2014.10.013>
- Tsou, H. R., Overbeek-Klumpers, E. G., Hallett, W. A., Reich, M. F., Floyd, M. B., Johnson, B. D., ... others. (2005). Optimization of 6, 7-disubstituted-4-(arylamino) quinoline-3-carbonitriles as orally active, irreversible inhibitors of human epidermal growth factor receptor-2 kinase activity. *J. Med. Chem*, *48*, 1107–1131. Retrieved from <http://pubs.acs.org/doi/abs/10.1021/jm040159c>
- Varshney, A., Sen, P., Ahmad, E., Rehan, M., Subbarao, N., & Khan, R. H. (2010). Ligand binding strategies of human serum albumin: How can the cargo be utilized? *Chirality*. <https://doi.org/10.1002/chir.20709>
- Wang, Z., Ho, J. X., Ruble, J. R., Rose, J., Rüker, F., Ellenburg, M., ... Carter, D. C. (2013). Structural studies of several clinically important oncology drugs in complex with human serum albumin. *Biochimica et Biophysica Acta*, *1830*(12), 5356–74. <https://doi.org/10.1016/j.bbagen.2013.06.032>
- Wei, J., Jin, F., Wu, Q., Jiang, Y., Gao, D., & Liu, H. (2014). Molecular interaction study of flavonoid derivative 3d with human serum albumin using multispectroscopic and molecular modeling approach. *Talanta*, *126*, 116–121. <https://doi.org/10.1016/j.talanta.2014.03.046>
- Zhou, H., Shi, X., Fan, Y., He, Z., Gu, W., Ye, L., & Meng, F. (2018). Interaction of Prussian blue nanoparticles with bovine serum albumin: a multi-spectroscopic approach. *Journal of Biomolecular Structure and Dynamics*, *36*(1), 254–261. <https://doi.org/10.1080/07391102.2016.1274273>
- Zsila, F. (2013). Subdomain IB is the third major drug binding region of human serum albumin: Toward the three-sites model. *Molecular Pharmaceutics*, *10*(5), 1668–1682. <https://doi.org/10.1021/mp400027q>